Structural Engineering and Mechanics, *Vol. 61, No. 1 (2017) 1-13*
DOI: https://doi.org/10.12989/sem.2017.61.1.001

Seismic repair of captive-column damage with CFRPs in substandard RC frames

Onur Tunaboyu* and Özgür Avşar[a]

Department of Civil Engineering, Anadolu University, 2 Eylul Campus, Eskisehir, Turkey

(Received March 11, 2016, Revised August 3, 2016, Accepted August 9, 2016)

Abstract. The effectiveness of the repair scheme for the damaged captive-columns with CFRPs (Carbon Fiber Reinforced Polymer) was investigated in terms of response quantities such as strength, ductility, dissipated energy and stiffness degradation. Two 1/3 scale, one-story one-bay RC (Reinforced Concrete) frames were designed to represent the substandard RC buildings in Turkish building stock. The first one, which is the reference specimen, is the bare frame without infill wall. Partial infill wall with opening was constructed between the columns of the second frame and this caused captive column defect. Severe damage was observed with the concentration of shear cracks in the second specimen columns. Then, the damaged members were repaired by CFRP wrapping and retested. For the three test series, similar reversed cyclic lateral displacement under combined effect of axial load was applied to the top of the columns. Overall response of the bare frame was dominated by flexural cracks. Brittle type of shear failure in the column top ends was observed in the specimen with partial infill wall. It was observed that former capacity of damaged members of the second frame was recovered by the applied repair scheme. Moreover, ultimate displacement capacity of the damaged frame was improved considerably by CFRP wrapping.

Keywords: repair; reinforced concrete; captive-column; CFRP; seismic

1. Introduction

Past destructive earthquakes demonstrate that the majority of the existing RC buildings in Turkey have poor seismic performance because of inadequate material quality, improper design applications and detailing in RC members in contrast with the earthquake resistant design principles (Yılmaz and Avşar 2013). In order to prevent the brittle type of behavior for RC buildings, Turkish Earthquake Code (TEC 2007) has imposed several limitations on the formation of structural irregularities in the plan and elevation as well as non-ductile applications such as captive column, short column, strong beam-weak column, etc. The buildings which have one or more irregularities mentioned in TEC (2007) can be exposed to moderate to severe damage after the earthquake. Depending on the level of the structural damage, the damaged building can either be demolished or repaired to satisfy the serviceability and the life-safety limit state. Through conducting an appropriate repairing technique, the seismic capacity of the damaged member can be recovered or even improved compared to its original capacity.

Brittle type of shear failure was commonly observed in captive columns after damaging earthquakes. Captive column defect is mostly due to the presence of openings for strip window provided in infill walls between the columns. Infill walls constrain the lateral displacement of the adjacent columns and hence clear height of the corresponding columns becomes shorter, which causes a substantial increase in the column stiffness. Consequently, such columns, namely captive columns, attract excessive amount of shear forces causing brittle shear failure before attaining the flexural capacity of the column.

There are several studies in the literature on the shear failure caused by the short and captive column defects. By considering the engineering, architecture and construction aspects, Guevara and Garcia (2005), presented an interdisciplinary solution to solve the short and captive column defects. The factors that might cause short-column and captive-column defects were explained in their work and shear failure damages were examined after various earthquakes. Moreover, the behavior of the frames with short-column and captive-column were explained in detail. Çağatay (2005) observed that all the outer columns of an industrial building were exposed to shear damages due to captive column effect during the 1998 Adana-Ceyhan Earthquake in Turkey. Although the concrete quality of the building was not in poor condition, the member shear reinforcements were widely spaced and detailed improperly. A finite element model was developed and the effect of the opening ratio on the infill wall was examined analytically. In order to eliminate the captive column effect, some practical applications were suggested. Pradhan, Maskey *et al*. (2014) discussed the stiffness behavior and the effect of shear in partially infilled RC frames. An equation was adopted for determining the stiffness behavior and the shear effect with partially infilled RC frame within the elastic limits. It was concluded that partially infilled walls improve the stiffness response but columns might be damaged by the

*Corresponding author, Ph.D. Candidate
E-mail: onurtunaboyu@anadolu.edu.tr
[a]Associate Professor, E-mail: ozguravsar@anadolu.edu.tr

http://www.techno-press.org/?journal=sem&subpage=8 ISSN: 1225-4568 (Print), 1598-6217 (Online)

high shear forces.

In case of column shear damage due to the formation of captive column, the corresponding building should be either demolished or repaired with an appropriate technique to meet the serviceability and life-safety criteria. In this study, it was planned to repair the damaged columns by FRP sheets. In the literature, although retrofitting RC members with FRPs were experimentally investigated and positive results were observed, the use of FRP for repair purposes is limited compared to retrofit applications. Ferrier, Avril *et al*. (2003) investigated the mechanical properties of RC beams wrapped with CFRP by a full-field optical method, called the grid method. They concentrated on the crack formation of the beams and emphasized that the performance of the beam improved due to strengthening both at the global and local scale. Altin, Anil *et al*. (2011) have outlined the retrofitting of shear deficient beams by using diagonal CFRP strips with and without anchorages. Their study proved that only the strips with anchorage could prevent the shear failure. Pan, Xu *et al*. (2007) conducted an experimental study to investigate the load carrying capacity of the slender RC columns wrapped with FRP. They concluded that the slenderness of the columns decreases by using CFRP sheets. Yalcin, Kaya *et al*. (2008) performed an experimental study for CFRP-retrofitted RC columns having some deficiencies like plain rebars, lap splice problems and insufficient stirrup spacing. The performance of the retrofitted lap spliced column was improved slightly; however, the performance was enhanced by welding the dowel rebars. Colomb, Tobbi *et al*. (2008) investigated the short columns in bridge piers with inadequate shear capacity. It was concluded that after retrofitting the short columns with FRP sheets, failure modes were changed. Ozcan, Binici *et al*. (2010) studied the flexural behavior of the CFRP-strengthened rectangular RC columns with plain bars, insufficient confining steel and low concrete strength. They concluded that the displacement capacity of the columns improved as high as three times that of the column without strengthening.

In the previous studies, the use of FRP for structural repair was proved to be effective in restoring the original or as-built capacity of the damaged structure. He, Yang *et al*. (2015) highlighted some of the differences between retrofit and repair of damaged bridge columns. They concluded that for earthquake-damaged RC columns without fractured longitudinal bars, jacketing with FRP proved to work well to restore both strength and ductility. Considering the structural repairing studies in the literature, Sheikh (2002) examined the performance of RC buildings after repairing them with FRP. Scaled tests were performed with slabs, beams and columns. The repair has been applied to the flexural cracks for the slabs, the shear cracks for the beams and the plastic hinge region for the columns. It was pointed out that flexural bending capacity of the damaged slabs increased; nevertheless, the behavior changed from the ductile flexural failure to a brittle mode of shear failure. After wrapping the beams with CFRP sheets, the brittle mode of shear failure changed to a ductile flexural failure. The seismic capacity of columns was increased by repairing with CFRP and GFRP (Glass Fiber Reinforced Polymer). Li and Kai (2011) investigated the seismic behavior of reinforced concrete interior beam column joints repaired by FRP with four non seismically detailed specimens. The repairing technique composed of epoxy injection in the cracks and externally bonded CFRP and GFRP sheets to improve the performance of the specimens that have flexural cracks on the beam near the column interface. By comparing the performance of the specimens they demonstrated that the repair of damaged RC joints with FRP is a cost-effective method. Yurdakul and Avşar (2015) concluded that after repairing the damaged RC beam-column joints with CFRP, the former capacities of the damaged members were recovered. Structural repairing of bridge columns by CFRPs were investigated in detail in the literature (Vosooghi and Saiidi 2013, He, Sneed *et al*. 2013a, He, Grelle *et al*. 2013b, Rutledge, Kowalsky *et al*. 2013, Yang, Sneed *et al*. 2015a, Yang, Sneed *et al*. 2015b). Vosooghi and Saiidi (2013) repaired the bridge columns using CFRP fibers, repair mortar and epoxy. After retesting the repaired columns on shake tables, they concluded that the strength and the displacement capacity of the standard columns were restored and those of substandard columns were upgraded to meet the seismic standards. He, Sneed *et al*. (2013a) focused on the rapid and effective repair methods for damaged bridges after an earthquake. In their study, CFRP sheets were used on the RC columns with different damage levels under combined cyclic loading including bending and torsion. He, Grelle *et al*. (2013b) developed a technique to rapidly repair severely damaged RC columns with externally-bonded CFRP for emergency service use. The effectiveness and limitations of the rapid repair technique was investigated with three half-scale severely damaged square RC bridge columns, which have buckled longitudinal bars, concrete cover spalling, and significant crushing of the concrete core. They have found the rapid repairing technique was successful for repairing the circular RC column strength if the bars of the columns have not fractured. Rutledge, Kowalsky *et al*. (2013) described a new repair technique that was related with the use of plastic hinge relocation to a higher location in the column in order to restore the strength and deformation capacity of RC bridge columns. They performed three large scale experiments with reversed cyclic testing and retested after repairing with CFRP sheets and carbon fiber anchors. Yang, Sneed *et al*. (2015a) conducted an experimental study to investigate the repairing of RC bridge columns with interlocking spirals and buckled and/or fractured longitudinal bars. The repair technique consists of two parts as, removing spirals, longitudinal bar segments in the plastic hinge region and replacing them with new bar segments that were externally bonded with CFRP. Yang, Sneed *et al*. (2015b) performed an experimental study with a RC bridge column that had buckled and fractured longitudinal bars by using externally bonded prefabricated CFRP laminates for emergency repair. In accordance with the study, the repair method was able to restore the lateral strength, stiffness and ductility of the column, however the performance of the repairing method achieved by the proper application of CFRP based on the bond provided by the epoxy.

In the previous studies, CFRP sheets were mostly used for retrofit and repair purposes for various RC structural members. Except for the study conducted by Jayaguru and Subramanian (2012), the seismic repair of captive column damage by FRPs was not investigated. Jayaguru and Subramanian (2012) conducted an experimental study on the repairing of captive column failure by GFRP. The objective of this study is to investigate the behavior of a frame having captive column defect and the effectiveness of the CFRP sheets used for repairing the heavily damaged captive columns. For this purpose, two 1/3 scale, one-story one-bay substandard RC frames were constructed. After testing the RC frame with partial infill wall, the damaged columns were repaired by CFRP sheets and retested with the same loading protocol. In order to examine the effectiveness of the repairing technique, the experimental results of the bare frame, the frame with captive column and the repaired frame were compared in terms of various response quantities such as strength, ductility, dissipated energy and stiffness degradation.

2. Experimental program

2.1 Test specimen details and material properties

Two 1/3 scale, one-story one-bay RC frames were constructed in the laboratory to represent the existing substandard RC buildings in the Turkish RC building stock, which have certain deficiencies such as low strength concrete, plain reinforcement bars, excessive spacing of ties and strong beam-weak column. The lateral load capacity of the test specimens is the fundamental response quantity in structural repairing of shear damaged columns. Since the effect of scaling has no considerable effect on the lateral load capacity of the specimens (Bazant 1993, Akin, Canbay *et al*. 2015), scale effect was not considered in this study. The first test specimen (CFRPE_01) is the bare frame, which is considered as the reference specimen. The reference specimen was constructed without infill wall. The second test specimen (CFRPE_02) was constructed with a partial infill wall between the columns leaving an opening at the top to cause captive column defect. The ratio of the opening height to the wall height is approximately 25%, which is a typical ratio for a strip window in the existing RC buildings. The partial infill wall was constructed by a mason, who is actively working in the building constructions for constructing infill walls. Therefore, the infill wall constructed in the test specimen CFRPE_02 represents the infill walls in the existing RC buildings. The geometric dimensions of the brick units and the overall infill wall dimensions were scaled in accordance with the scale of the RC frame. After the severe damage was observed with the same loading history of the reference specimen, the damaged CFRPE_02 specimen was repaired with CFRP sheets and the repaired specimen was named as CFRPE_03. Before repairing the CFRPE_03 specimen, the damaged infill wall was removed from the frame and the damaged columns were wrapped with CFRP sheets. After the repair, no infill wall was constructed between the columns of CFRPE_03 to prevent the recurrence of the captive column defect. In real life applications, in case of

Table 1 Properties of the test specimens

	Infill Wall	Ratio of the opening height to the wall height	CFRP
 CFRPE_01	-	N/A	-
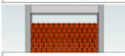 CFRPE_02	+	1/4	-
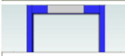 CFRPE_03	-	N/A	+

any requirement for the construction of infill wall with the opening resulting in a captive column defect, the partial infill wall should be isolated from the frame with sufficient amount of gap between the frame and the infill wall provided that the out-of-plane failure of the wall is prevented by taking relevant precautions. This will enable the frame to behave like a bare frame without formation of captive column defect. With this approach in mind, infill wall was removed and not reconstructed in the repaired specimen. All the three tested specimens were subjected to similar lateral displacement loading protocol and vertical loading. Some of the structural properties of the tested specimens are listed in Table 1.

Fig. 1 illustrates the geometric and reinforcement details of the tested specimens with the frame aspect ratio of 0.58. The aspect ratio is the ratio of frame height (h) to its width (L). All the specimens have the same column and beam dimensions of 100 mm×150 mm and, 150 mm×150 mm respectively. The geometry and the cross-section details of the one-story one-bay RC frames were obtained from the study of Akin, Canbay *et al*. (2015). The foundations of the test specimens were designed much stiffer than the columns to provide a fully restraint support condition for the column bottom ends. The foundation was connected to the strong floor with six bolts with the purpose of restricting any displacement.

Longitudinal reinforcements have a diameter of 8 mm, which corresponds to a reinforcement ratio of 1.3% both for columns and beam. Additionally, plain bars, which had a diameter of 4 mm and spaced at 100 mm, were used as transverse reinforcement for all members. Bond-slip behavior dominates the overall response of the substandard RC frames when plain round bars are used (Ilki, Bedirhanoglu *et al*. 2011, Akın, Canbay *et al*. 2015). In order to avoid premature bond-slip failure, continuous reinforcements were used in all members. Except for the lap splice, the details shown in Fig. 1 are representative of existing construction practice in the substandard RC frames in Turkey. Several material tests were conducted on the reinforcement samples to obtain the material properties of the reinforcement steel. The average values of yield strength, tensile strength and modulus of elasticity were determined as 311 MPa, 417 MPa and 200 GPa, respectively. The maximum aggregate size is selected to be 12 mm for the concrete mixture design of low concrete strength. The target compressive strength of concrete was selected to be 10 MPa in order to represent the low concrete

Table 2 Compressive strength of concrete

		Compressive Strength, f_c (MPa)		Compressive Strength, f_c^* (MPa)	
		Samples	Average	Samples	Average
CFRPE_01	1	7.9	7.9	11.4	10.9
	2	7.9		11.5	
	3	8.0		9.9	
CFRPE_02	1	9.0		10.2	
	2	9.3	9.1	8.6	9.4
	3	8.9		9.4	

f_c : Standard cylindrical concrete compressive strength at 28 days after casting
f_c^* : Standard cylindrical concrete compressive strength on the date of experiment

Fig. 2 Excessive shear cracks on the captive columns before repairing (CFRPE_02)

(a) Rounding corners

(b) Injecting chemical anchorage

(c) Applying repair mortar

(d) Applying primer epoxy coater

(e) Application of epoxy based repair and anchorage mortar

(f) Wrapping CFRP sheets with saturant material

Fig. 3 Repairing procedure for the damaged captive columns

strength. Although the compressive strength of concrete used in the test specimens is very low, 10 MPa represents the poor material quality in the existing substandard RC buildings, which is a common phenomenon in Turkey (Avşar and Tunaboyu 2014). The concrete compressive strength of the specimens is summarized in Table 2, for the compressive strength at 28 days after casting and on the date of experiment. The unidirectional CFRP sheets were used in the repair of CFRPE_03. Some of the geometric and material properties of the CFRP sheets were provided by the manufacturer. The thickness is 0.111 mm, the modulus of elasticity is 230 GPa, the ultimate tensile strength is 4900 MPa and the ultimate strain is 2.10%. Before wrapping the columns with CFRP sheets, the shear cracks at the top of the columns were filled by injecting the chemical anchorage based on an epoxy acrylate resin. After injecting the chemical anchorage, a repair mortar with a 28-day compressive strength of 40 MPa was used to minimize damage potential in the same damaged region of the repaired test specimen. A primer epoxy coater, which has a

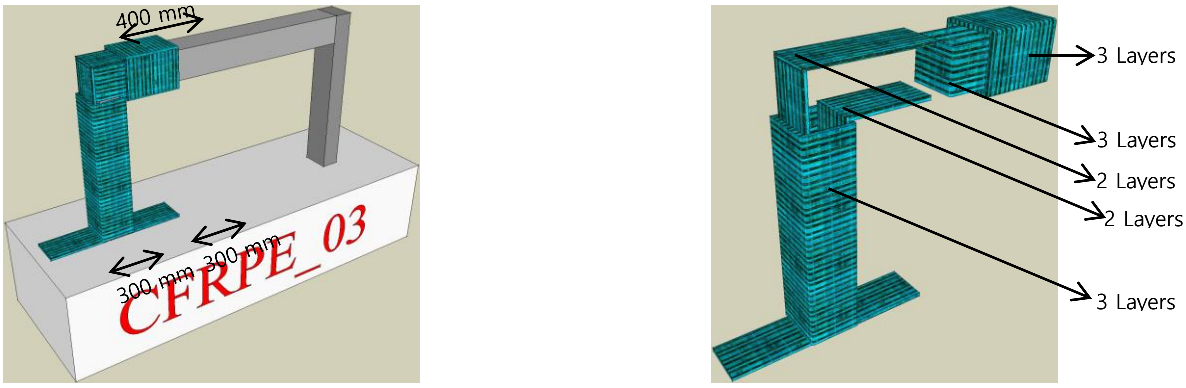

Fig. 4 Schematic representation of CFRP sheets

20 MPa flexural bending capacity, was applied before the application of CFRP sheets. Another epoxy based repair and anchorage mortar, which has 75 MPa compressive strength, was applied to obtain a smooth surface. Finally, a saturant material with a 60 MPa compressive strength was used based on the recommendation of the manufacturer.

2.2 Structural repair design

Depending on several constraints such as cost, applicability, workmanship, etc., certain techniques can be applied for repairing the damaged structural members. Based on the previous studies, it was decided to wrap the damaged captive columns by CFRP sheets, which was proved to be one of the effective techniques for retrofitting and repairing. Fayyadh and Razak (2014) described the advantages of CFRP as high tensile strength, low weight, and low installation cost. Accordingly, CFRP sheets were used to upgrade the seismic performance of repaired specimen in terms of stiffness, strength and energy dissipating capacity. After the occurrence of severe damage due to the shear cracks in the captive columns under the reversed cyclic lateral displacement, repairing procedure was applied to the CFRPE_02 specimen (Fig. 2).

Before the application of CFRP, the corners of the columns and beam members were rounded with a radius of 10 mm to get smooth corners for the RC sections (Fig. 3(a)). Otherwise, sharp corners of the RC sections can cause tearing of CFRP sheets, which can reduce the effectiveness of the repairing technique.

To fill the large shear cracks, observed at the top of the columns, an epoxy acrylate resin called chemical anchorage was injected into the cracks (Fig. 3(b)). The next step of the repairing procedure is the application of repair mortar in the place of spalled concrete (Fig. 3(c)). A primer epoxy coat at around 0.1 mm was used to provide an efficient adhesion between the concrete and epoxy based repair-anchorage mortar (Fig. 3(d)). The last step before the CFRP wrapping is both to cover the repairing parts with an epoxy based repair-anchorage mortar for repairing the wide cracks and to provide certain level of bonding between the repaired specimen and the CFRP sheets (Fig. 3(e)). Finally, the beam and the columns were wrapped by CFRP sheets with an epoxy resin before hardening the repair-anchorage mortar. The resin is used for establishing connection between the CFRP sheets and the repair-anchorage mortar. Proper application of CFRP increases the flexural and shear capacity of the applied members (Fig. 3(f)).

Although the main damage mechanism for the test specimen CFRPE_02 was the brittle type of shear failure at the captive columns, hairline shear and flexural cracks were observed in the beam and beam-column joints. Three layers of CFRP sheets with a width of 150 mm were placed over the joint regions to repair the hairline cracks on the joints. To improve the flexural capacity of the columns, two layers of CFRP sheets were placed longitudinally over the front and backside of the two columns along the direction of the loading (Fig. 4). The 150 mm width longitudinal CFRP sheets were extended over the foundation and the beam by 300 mm. The CFRP sheets, which were used for improving the shear capacity of the columns and confining purposes, were placed with three layers continuously through the columns in transverse direction. The beam was strengthened against the increased shear demands with three layers of 300 mm CFRP sheets applied in the transverse direction from the joint at both ends.

Xie, Liu *et al*. (2005) discussed the shear capacity of RC columns strengthened with CFRP sheets. Based on their analyses results, it is emphasized that the axial load ratio, the shear span/depth ratio and the number of CFRP sheet layers affect the column shear capacity. They suggest a design method used to calculate the shear capacity of RC columns confined with CFRP. For the CFRP sheet configuration employed in this study, the shear capacity of the column was calculated according to the Eq. (1) and determined as 22 kN without considering the contribution of the concrete and the stirrups of the damaged captive columns.

$$V_f = \frac{2.n_f.t_f.w_f.E_f.\varepsilon_f.d}{s_f} \tag{1}$$

2.3 Instrumentation, test system and loading procedure

Quasi-static cyclic tests were conducted to obtain the several response quantities such as strength, ductility, dissipated energy and stiffness degradation. The test system was instrumented to record strain values at critical

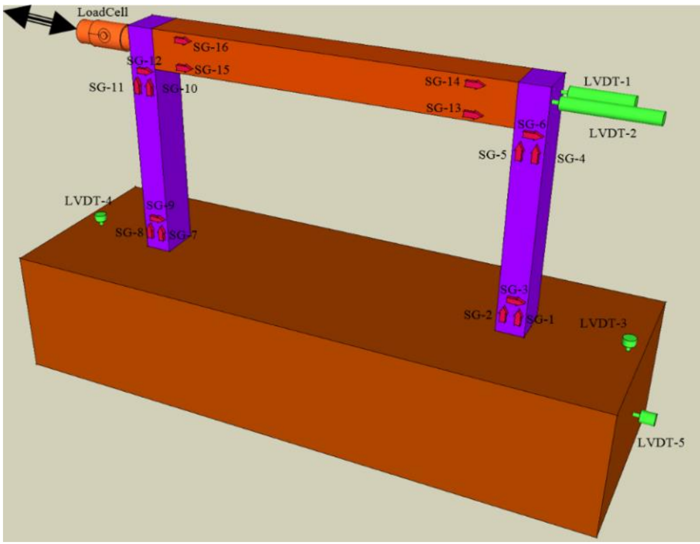

Fig. 5 Instrumentation of the tested specimens

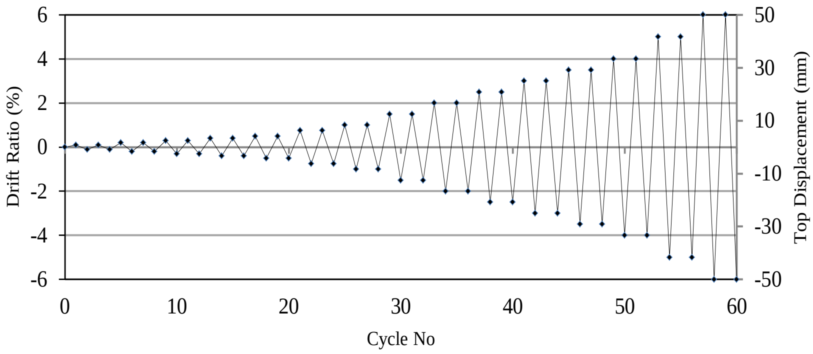

Fig. 6 Displacement loading protocol

reinforcement rebars, displacements and lateral load. These data were used to calculate the response quantities. Two Linear Variable Displacement Transducers (LVDT) were used to get the top displacement values at the beam level. A load cell was installed to get the positive (push) and negative (pull) load values at the same level with LVDTs. Two LVDTs were placed on the rigid foundation to measure the base rotation and one LVDT to obtain the horizontal movement at the base. There were four strain gauges on the longitudinal rebar of the beam, eight strain gauges on the longitudinal rebar and four strain gauges on the stirrups of columns to record the axial deformations in the bars (Fig. 5). After conducting the test for CFRPE_02, the strain gauges were mostly reached their capacity and/or damaged. All the strain gauges and their cables were removed from the repaired specimen during the application of structural repairing for CFRPE_03. Therefore, no yielding information could be obtained for the repaired specimen.

All the specimens were tested under the combined action of constant column axial load and reversed cyclic lateral displacement. The constant vertical load, which is 10% of the axial load capacity of the columns, was determined by the minimum axial load for the columns according to TEC (2007). The reason for using the minimum level of axial load is not to increase the shear capacity of the columns. The axial load was applied by the weight of the steel blocks which were directly placed on the top of the columns to transfer the axial load to each of the column equally. Direct application of axial load by the steel blocks enables constant axial load on the columns, which is independent of the lateral displacement of the frame. Elastomeric bearings were employed between the steel blocks and the top ends of the columns to prevent the rigidity transfer from the steel blocks to the RC frame. Reversed cyclic lateral displacement was applied by a computer controlled hydraulic actuator at the beam level. Each drift ratio cycle was repeated twice as represented in Fig. 6.

3. Test results

3.1 Observed damage

The first frame (CFRPE_01) was the reference frame without infill wall. The maximum lateral load was measured as 11.1 kN and the test was ended at the top displacement of 50 mm (6% drift ratio). The first crack was observed at the joint at 0.1% drift ratio. At the same cycle, a crack occurred between the column and the foundation connection. During the test, flexural behavior dominated the

(a) CFRPE_01 (b) CFRPE_02 (c) CFRPE_03

Fig. 7 Damage pattern of the test specimens at 2% drift ratio

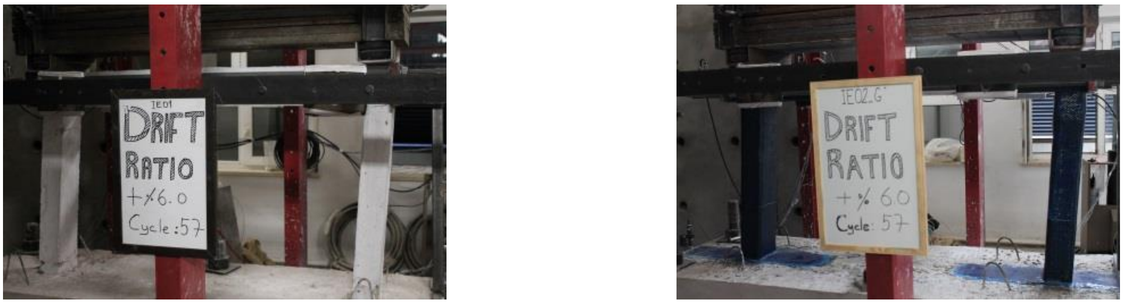

(a) CFRPE_01 (b) CFRPE_03

Fig. 8 Damage pattern of the test specimens at 6% drift ratio

overall response of CFRPE_01 with the concentration of the flexural cracks mostly in the columns. Under constant axial load and reversed cyclic lateral displacement, a ductile behavior was observed with limited lateral load capacity compared to the lateral load capacities of the other specimens.

The second frame (CFRPE_02) was the test specimen with captive column defects. Due to the increased strength and stiffness with the presence of the partial infill wall, the maximum lateral load was obtained as 28.2 kN, which is more than 2.5 times the lateral load capacity of the reference frame. Flexural cracks started to occur from the beginning of the experiment at both columns and joints. The separation of the infill walls from the columns was observed at 0.1% drift ratio. When the drift ratio reached to 0.5%, shear cracks occurred in the captive columns. A sudden drop in the lateral capacity of the frame was observed at 1.0% drift ratio. Because of the severe damage in the captive columns in the succeeding drift ratios, the test for CFRPE_02 was ended at the displacement of 16 mm (2% drift ratio) due to safety concerns. After the expected captive column damage occurred and the excessive shear cracks were monitored, the test was terminated. Although the infill wall with opening in the frame caused a considerable amount of increase in the lateral load capacity of the frame in the first cycles, partial infill wall constrained the lateral displacement of the captive column and caused a brittle type of column shear failure in the succeeding cycles.

After the damage occurred in CFRPE_02, it was repaired with CFRPs and retested as CFRPE_03, which is the repaired frame. The maximum lateral load of CFRPE_03 was recorded as 21.8 kN, which is almost twice the lateral load capacity of the reference specimen. The test was ended at the top displacement of 50 mm (6% drift ratio). Since the columns, beam and joints of the frame were wrapped with CFRPs, crack formation in the RC members as well as the rupture of the CFRP sheets could not be monitored apparently. After 4% drift ratio, some of the inner CFRP layers were ruptured, which caused strength deterioration specifically in the second cycle for the 4.4% drift ratio in the positive direction and in the first cycle of the 4.3% drift ratio in the negative direction (Fig. 10(c)). Although a ductile behavior was observed up to 4% drift ratio, a sharp decrement occurred in the strength as a result of rupture in the inner layer of CFRP sheets.

The damage pattern of all the test specimens at 2% drift ratio are shown in Fig. 7. Nevertheless, only CFRPE_01 and CFRPE_03 specimens can displace up to 6% drift ratio. The views from both specimens are presented in Fig. 8 to demonstrate the damage pattern at the ultimate displacement.

3.2 Base shear-Lateral displacement relations

In order to determine the lateral load as well as the displacement capacity of the tested specimens, base shear force vs. top displacement graphs were plotted as given in Fig. 10. Priestley, Verma *et al*. (1994) explained some predictive shear strength equations for RC columns. Similarly, according to Turkish Earthquake Code (TEC 2007), the total shear capacity of the columns is computed as 24 kN with Eq. (2), which corresponds to the lateral force capacity of CFRPE_01 specimen. The tensile strength values of the concrete were taken as 1.2 MPa and 1.1 MPa for CFRPE_01 and CFRPE_02, respectively. As shown in Fig. 10(a) the columns did not reach their shear capacity

(a) CFRP delamination of column (b) CFRP swelling (c) Flexural crack in the beam

Fig. 9 Failure pattern of CFRP

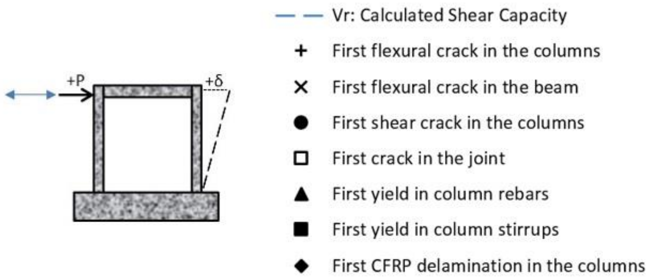

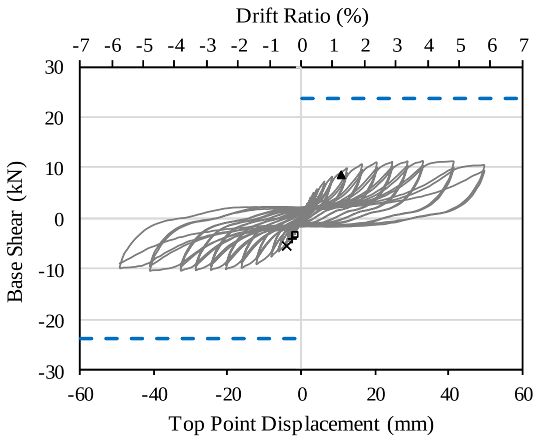

(a) CFRPE_01

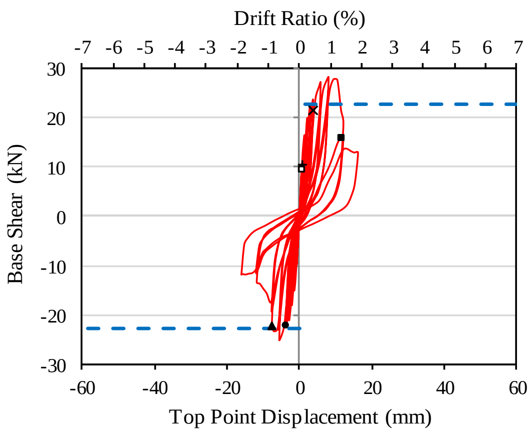

(b) CFRPE_02

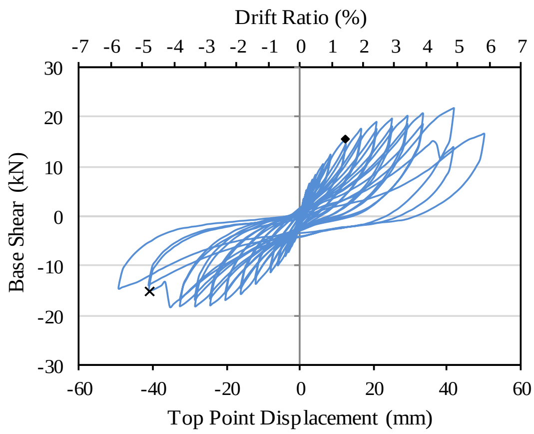

(c) CFRPE_03

Fig. 10 Hysteretic loops of the specimens

and shear crack did not occur in CFRPE_01 specimen. The first flexural crack in the joints, columns and beam was observed at the drift ratio of 0.2%, 0.3% and 0.5%, respectively. Only longitudinal rebars of the columns yielded and the first yield point was observed at 1.3% drift ratio through the strain gauge measurements.

$$V_r = \left[0.52 \cdot f_{ct} \cdot b_w \cdot d \cdot \left(1 + 0.07 \cdot \frac{N_d}{A_c}\right)\right] + \left[\frac{n \cdot A_0}{s} \cdot f_{yw} \cdot d\right] \quad (2)$$

According to Fig. 10(b), the ultimate lateral load of CFRPE_02 was obtained as 28.2 kN and 25.0 kN in the positive and negative directions, respectively. A sudden drop in the lateral load was observed after attaining the peak lateral load values due to the shear damage at the captive columns. The code specified shear capacity of the columns was calculated as 23 kN according to Eq. (2). The calculated shear capacity is in good agreement with the lateral load capacity obtained from the test.

Due to the reduction in the effective length of the

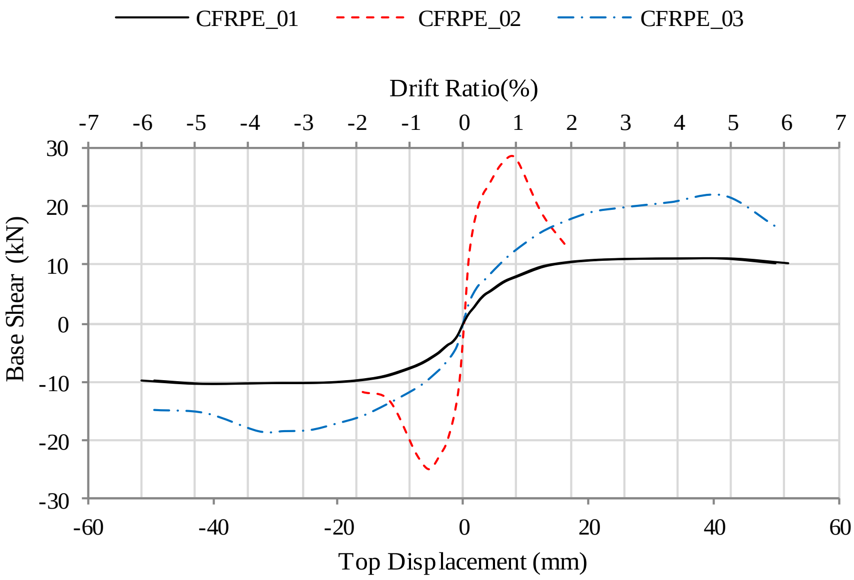

Fig. 11 Envelope curves for hysteretic loops

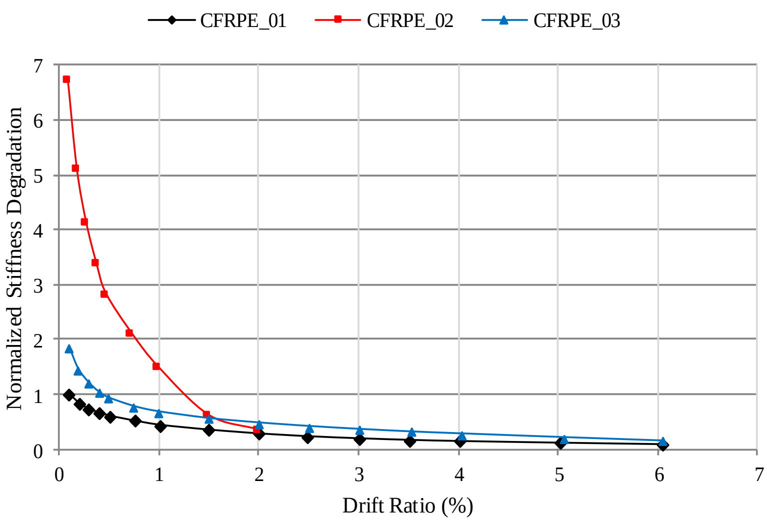

Fig. 12 Stiffness degradation

captive column by the partial infill wall, the stiffness of the captive column increased considerably. Therefore, most percentage of the lateral shear force was taken by the column close to the applied load (due to captive column effect). As a result, the captive column attracted a shear demand exceeding its shear capacity. This phenomenon caused the shear failure of the columns, which violates the capacity design principles defined in TEC (2007).

In the test specimen CFRPE_02, the first flexural cracks were observed in the columns and joints at 0.1% drift ratio, whereas it was at the 0.5% drift ratio in the beam. At 0.5% drift ratio the first shear crack in the column of CFRPE_02 was observed due to the captive column defect. Strain gauge measurements imply that the first yield occurred at 0.9% drift ratio for the longitudinal reinforcement bars and 1.4% for the stirrups in the columns.

Since the section cracks have remained under the CFRP layers, they could not be apparently seen in the CFRPE_03 specimen. The first delamination at the interface of the column and joint CFRP sheets in the column initiated at 1.5% drift ratio as seen in Fig. 9(a). In Fig. 9(b) the swelling of CFRP sheets was observed as the drift ratio increased. After the 5% drift ratio, flexural cracks were observed at the middle part of the beam, which was not wrapped with CFRP (Fig. 9(c)). In Fig. 10(c) two sudden decrement of load values were monitored when the target drift ratio was 4% in the negative direction. At that point, a sound similar to the fracture sound was heard. However, the fracture of the CFRP sheets could not be apparently observed from the outer CFRP layers of the repaired specimen.

Lateral load capacity is one of the important parameters to discuss the effectiveness of the applied repairing technique. Response envelope curves were used to comment on the strength characteristics of the test specimens. Envelope curves were constructed by combining the ultimate lateral load values at the target displacement

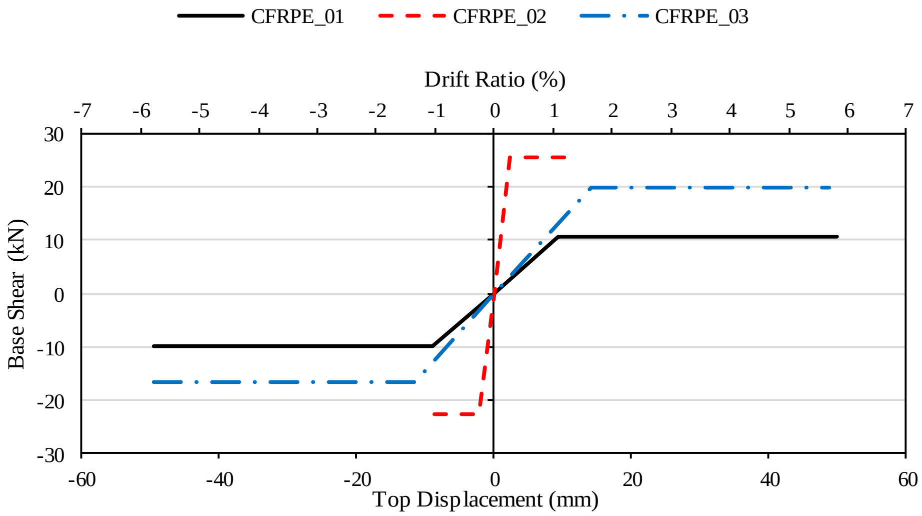

Fig. 13 Idealized bi-linear representation of the envelope curves

Table 3 Parameters of the idealized bi-linear force-displacement curves of the tested specimens

	d_y (mm)	d_{max} (mm)	δ_y (%)	δ_{max} (%)	V_y (kN)	Ductility
CFRPE_01	9.2	49.9	1.12	6.05	10.7	5.4
CFRPE_02	2.4	10.7	0.29	1.30	25.5	4.5
CFRPE_03	14.1	48.6	1.70	5.89	20.0	3.5

points at the first peak of each cycle, as seen in Fig. 11. It can be inferred that the strength of the repaired specimen (CFRPE_03) is greater than the one for reference specimen (CFRPE_01). However, if the results were compared with the second specimen (CFRPE_02), the repaired specimen had a 23% lower strength value because of the contribution of partial infill wall in CFRPE_02. For CFRPE_01, CFRPE_02 and CFRPE_03 specimens, the ultimate strengths were observed at 4%, 1% and 5% drift ratio, respectively. Except for the CFRPE_02 specimen, the other two specimens can be displaced up to the test displacement limits. Nevertheless, the second test had to be finalized at 2% drift ratio due to safety concerns.

3.3 Stiffness degradation

As the lateral displacement increased, lateral stiffness of the test specimens decreased very rapidly due to the formation of cracks and imposed plastic deformations (Fig. 12). The first step of specifying stiffness degradation was to determine the peak-to-peak stiffness for each displacement cycle. Peak-to-peak stiffness was defined as the slope of the line between peak lateral load values corresponding to the displacement value for positive and negative cycles. Then the peak-to-peak stiffness for each cycle was normalized with respect to the one for reference specimen for the first cycle. The normalized peak-to-peak stiffness versus drift ratio curves are shown in Fig. 12. As it can be observed from Fig. 12, CFRPE_02 specimen has the highest initial stiffness value due to the lateral rigidity of the partial infill wall for the first cycle, and also a rapid reduction in stiffness is observed in this specimen. CFRPE_03 specimen has greater stiffness value compared to the reference specimen. However, after 2% drift ratio, both have very close stiffness values. Although the initial stiffness of the repaired specimen without infill wall is lower than the frame with partial infill wall, its stiffness is almost twice the initial stiffness of the reference specimen. This implies that CFRP wrapping can improve the stiffness of the damaged RC frames even more than its original stiffness values for the bare frame.

3.4 Idealized bi-linear curves

Park (1989) calculated the yield displacement and the ductility of a frame with an idealized elasto-plastic load-displacement relation. Fig. 13 represents the idealized bi-linear form of envelope curves for all test specimens. The inclined part of the graphs represents the equivalent initial stiffness of the RC frames. According to FEMA 356 (2000), equivalent initial stiffness is defined as the slope of a line connecting the origin and the point that corresponds to the 60% of the ultimate load on the increasing part of the envelope curve. The post-yield region of the graph was extended up to the displacement value at which the lateral load reduces to 80% of the ultimate load on the descending part of the envelope curve. In order to specify the yield point, an iterative procedure was employed such that the areas under the idealized bi-linear and envelope curve are equal to each other.

Yield (d_y) and ultimate displacement (d_{max}) and their corresponding drift ratios (δ_y & δ_{max}), idealized lateral load (V_y) and ductility of the tested specimens are listed in Table 3. CFRPE_02 specimen reached its ultimate lateral load

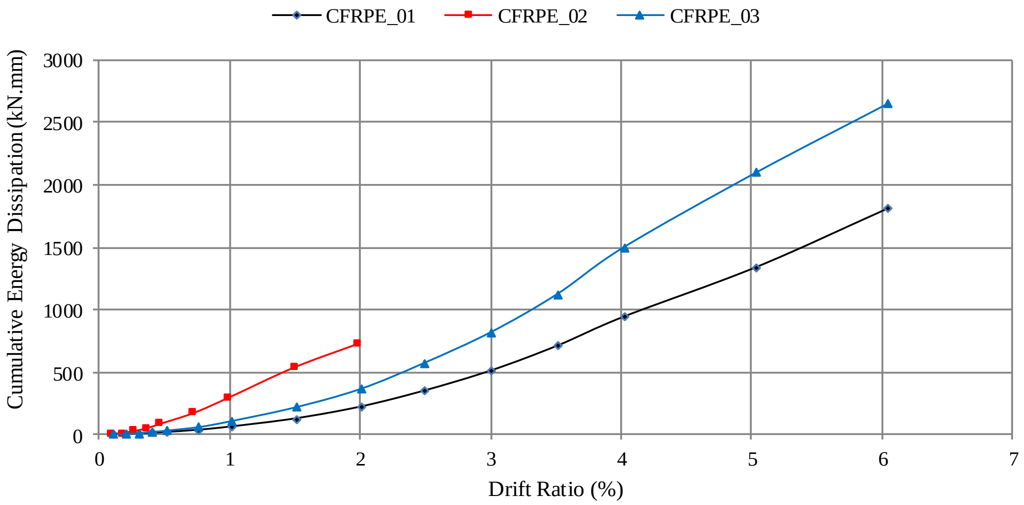

Fig. 14 Cumulative energy dissipation capacity of the tested specimens

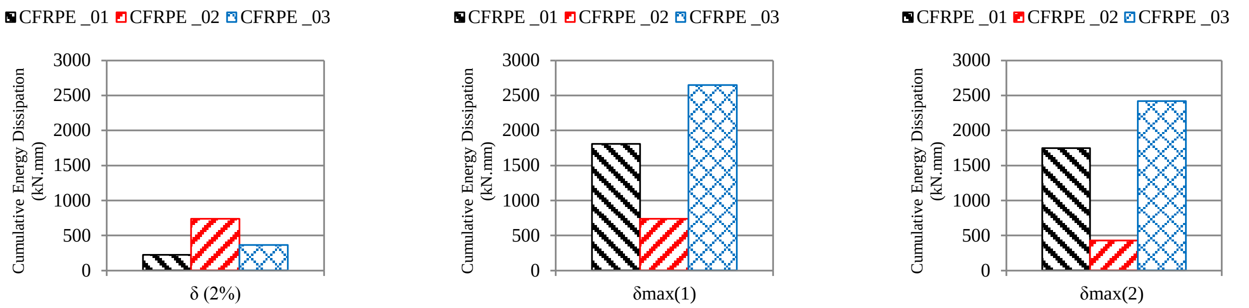

(a) 2% Drift Ratio

(b) Maximum displacement value from the test

(c) Maximum displacement value from the idealized curve

Fig. 15 Cumulative energy dissipation comparison

capacity at 0.29% drift ratio, and ultimate drift ratio was observed at 1.30%, which corresponds to the 20% decrement in the ultimate lateral load of the specimens. The ductility value for CFRPE_02 was calculated to be higher than the ductility of the repaired specimen (CFRPE_03). These ductility values do not represent the actual behavior of the tested specimens. Due to the excessive shear damage on the captive columns of CFRPE_02, the test had to be terminated at 2% drift ratio. Yield displacement plays a very important role in the calculation of ductility parameter. Due to the high rigidity of the partial infill wall in CFRPE_02, the yield displacement for this specimen was calculated to be much smaller compared to the other specimens. Although the repaired specimen has the lowest ductility, its ultimate displacement value is almost five times greater than the one for CFRPE_02 specimen. For this reason, both ductility and displacement capacities of the specimens should be taken into account in comparing the seismic response of the tested specimens.

3.5 Energy dissipation

The energy dissipation capacities of the tested specimens in each cycle were calculated as the area enclosed by the first cycle of the corresponding hysteretic loops. The cumulative energy dissipation was calculated by the summation of the areas of the hysteretic loops up to the corresponding drift ratios. Fig. 14 presents the relation between cumulative energy dissipation vs. drift ratio of the specimens. At 2% drift ratio, CFRPE_02 specimen has the greatest dissipated energy capacity and the remaining specimens have almost similar capacities. When Fig. 14 is examined for 6% drift ratio, it can be concluded that the repaired specimen has more energy dissipation capacity than the reference specimen.

Fig. 15 presents the comparisons in the dissipated energy capacity among the three specimens at specific drift ratio values for 2%, $\delta_{max}(1)$ and $\delta_{max}(2)$. $\delta_{max}(1)$ is the maximum displacement that can be applied to the specimens. $\delta_{max}(2)$ is the displacement which corresponds to a 20% reduction in the ultimate lateral load on the descending part of the hysteresis curve (the ultimate displacement of the idealized bilinear curves in Fig. 13). It is clearly seen in Fig. 15 that CFRPE_03 specimen has greater dissipated energy capacity for all comparisons except for the 2% drift ratio. CFRPE_02 specimen has the highest energy dissipated capacity at 2% drift ratio with the contribution of the partial infill wall. For all comparisons, the repaired specimen has greater dissipated energy capacity than CFRPE_01.

4. Conclusions

This study mainly focused on the effectiveness of CFRP sheets for repairing the damaged captive columns, which were exposed to shear damages. In order to investigate the effectiveness of the repair scheme in terms of various response quantities, three 1/3 scale specimens were tested under the combined effect of a constant axial load and lateral reversed cyclic displacement. The same lateral displacement protocol was applied for the three specimens; bare frame, frame with the partial infill wall and repaired frame without infill. To represent the substandard RC buildings in the Turkish building stock, low strength concrete and improper reinforcement detailing were used in the test specimens. The first specimen displayed a ductile behavior with limited lateral strength. Non-ductile behavior of captive column defect was observed in the second frame with a partial infill wall. Wide shear cracks were monitored in the captive columns for this frame. The test was terminated for safety concerns after 2% drift ratio due to the severe damage in the captive columns. The specimen was then repaired with CFRP sheets by wrapping around the columns, joints and beam in order to investigate the effectiveness of the repairing scheme. No infill wall was constructed in the repaired specimen to prevent the recurrence of the captive column defect. The third specimen displayed a ductile behavior up to 4% drift ratio and a sudden decrement in strength was observed after the rupture in several CFRP sheets. The following conclusions can be drawn from the experimental evaluations.

- Partial infill walls adversely affect the seismic performance of the RC buildings by causing captive column defects. Captive columns attract excessive amount of lateral load which can exceed its shear capacity and they can expose to severe damage resulting from the wide shear cracks. Depending on the damage level in the captive columns, the structural system can be further in service if an effective repairing is applied and certain precautions are taken (e.g., partially infill wall can be isolated from the frame) to prevent the recurrence of the captive column defect in the repaired specimen. In this study, CFRP wrapping on the damaged captive columns was found to be effective in terms of several response parameters such as strength, displacement capacity, dissipated energy and stiffness degradation.
- The repaired specimen without infill wall has 23% lower lateral load capacity than the lateral load capacity of the second specimen with the partial infill wall. On the other hand, the lateral load capacity of the repaired specimen without infill wall is almost twice the one for original bare frame. This result reveals that repairing the damaged captive columns with CFRPs and without infill wall can enhance the performance of its original undamaged bare frame considerably in terms of lateral load capacity.
- Although the test of CFRPE_02 was terminated at 2% drift ratio due to the severe damage in the captive columns, the repaired specimen can 6% drift ratio without any excessive strength deterioration. Although the columns were damaged severely in the previous test, wrapping them by CFRP sheets improved their ultimate displacement capacity considerably.
- Due to the contribution of infill stiffness, CFRPE_02 specimen has 7 times higher initial stiffness than the reference specimen and 3.5 times higher initial stiffness than the repaired specimen. The repaired specimen has 2 times higher initial stiffness than the reference specimen. A severe stiffness degradation occurred at the CFRPE_02 specimen after the formation of shear cracks in the captive columns. It was also observed that after the 2% drift ratio, the stiffness of the specimens became closer to each other.
- CFRPE_02 specimen has a good energy dissipation capacity up to 2% drift ratio, but after that point energy dissipation capacity is almost lost because of the severe damage in the columns. The cumulative energy dissipation capacity in the last step of the tests shows that the repaired specimen with CFRPs has more than 40% energy dissipation capacity than the one for the reference specimen. Therefore, it can be concluded that the repairing technique is effective in terms of energy dissipation capacity.
- The experimental results show that seismic repair of captive-column damage with CFRP sheets in substandard RC frame can rehabilitate and even improve the response of the undamaged bare frame. In case of captive column damage, damaged structural system can be serviceable after applying the proposed repairing scheme by the CFRP sheets and isolating the partial infill wall from the frame to prevent the recurrence of the captive column defect.

Acknowledgments

The research described in this paper was financially supported by Anadolu University Scientific Research Projects Commission [Grant Number: 1303F055].

References

Akin, E., Canbay, E., Binici, B. and Özcebe, G. (2015), "Scale effect on CFRP strengthening of infilled reinforced concrete frames", *J. Adv. Concrete Tech.*, **13**, 355-366.

Altin, S., Anil, Ö., Ocakli, Ö. and Kopraman, Y. (2011), "Retrofitting of shear damaged RC beams using diagonal CFRP strips", *J. Reinf. Plast. Compos.*, **30**(17), 1495-1507.

Avşar, Ö. and Tunaboyu, O. (2014), "Influence of structural walls on the seismic performance of RC buildings during the May 19, 2011 Simav Earthquake in Turkey", *J. Perform. Constr. Facil.*, **28**(4), 04014016.

Bazant, Z. (1993), "Scaling laws in mechanics of failure", *J. Eng. Mech.*, **119**(9), 1828-1844.

Çağatay, İ. (2005), "Failure of an industrial building during a recent earthquake in Turkey", *Eng. Fail. Anal.*, **12**, 497-507.

Colomb, F., Tobbi, H., Ferrier, E. and Hamelin, P. (2008), "Seismic retrofit of reinforced concrete short columns by CFRP materials", *Compos. Struct.*, **82**, 475-487.

Fayyadh, M.M. and Razak, A.H. (2014), "Analytical and experimental study on repair effectiveness of CFRP sheets for

RC beams", *J. Civil Eng. Manage.*, **20**(1), 21-31.
FEMA-356 (2000), Prestandard and commentary for the seismic rehabilitation of buildings, Washington, D.C.
Ferrier, E., Avril, S., Hamelin, P. and Vautrin, A. (2003), "Mechanical behavior of RC beams reinforced by externally bonded CFRP sheets", *Mater. Struct.*, **36**(8), 522-529.
Guevara, L.T. and Garcia, L. (2005), "The captive- and short-column effects", *Earthq. Spectra* **21**(1), 141-160.
He, R., Grelle, S., Sneed, L.H. and Belarbi, A. (2013b), "Rapid repair of a severely damaged RC column having fractured bars using externally bonded CFRP", *J. Compos. Struct.*, **101**, 225-242.
He, R., Sneed, L.H. and Belarbi, A. (2013a), "Rapid repair of severely damaged RC columns with different damage conditions: An experimental study", *Int. J. Concrete Struct. Mater.*, **7**(1), 35-50.
He, R., Yang, Y. and Sneed, L.H. (2015), "Seismic repair of reinforced concrete bridge columns: a review of research findings", *J. Bridge Eng.*, ASCE, **20(**12), 04015015.
Ilki, A., Bedirhanoglu, I. and Kumbasar, N. (2011), "Behavior of FRP-retrofitted joints built with plain bars and low-strength concrete", *J. Compos. Constr.*, **15**, 312-326.
Jayaguru, C. and Subramanian, K. (2012), "Retrofit of RC frames with Captive-Column defects", *KSCE J. Civil Eng.*, **16**(7), 1202-1208.
Li, B. and Kai, Q. (2011), "Seismic behavior of reinforced concrete interior beam-wide column joints repaired using FRP", *J. Compos. Constr.*, **15**(3), 327-338.
Ozcan, O., Binici, B. and Ozcebe, G. (2010), "Seismic strengthening of rectangular reinforced concrete columns using fiber reinforced polymers", *Eng. Struct.*, **32**, 964-973.
Pan, J.L., Xu, T. and Hu, Z. (2007), "Experimental investigation of load carrying capacity of the slender reinforced concrete columns wrapped with FRP", *Constr. Build. Mater.*, **21**(11), 1991-1996.
Park, R. (1989), "Evaluation of ductility of structures and structural assemblages from laboratory testing", *Bull. NZ Nat. Soc. Earthq. Eng.*, **22**, 155-156.
Pradhan, P.M., Maskey, R.K. and Pradhan, P.L. (2014), "Stiffness behavior and shear effect in partially infilled reinforced concrete frames", *J. Earthq. Eng.*, **18**(4), 580-588.
Priestley, M.J., Verma, R. and Xiao, Y. (1994), "Seismic shear strength of reinforced concrete columns", *J. Struct. Eng.*, **120**(8), 2310-2329.
Rutledge, S.T., Kowalsky, M.J., Seracino, R. and Nau, J.M. (2013), "Repair of reinforced concrete bridge columns containing buckled and fractured reinforcement by plastic hinge relocation", *J. Bridge Eng.*, **19**(8), A4013001-1
Sheikh, S.A. (2002), "Performance of concrete structures retrofitted with fibre reinforced polymers", *Eng. Struct.*, **24**(7), 869-879.
Turkish Earthquake Code (2007), Specification for buildings to be built in seismic zones, Ankara, Turkey.
Vosooghi, A. and Saiidi, M.S. (2013), "Shake-table studies of repaired reinforced concrete bridge columns using carbon fiber-reinforced polymer fabrics", *ACI Struct. J.*, **110**(1), 105-114.
Xie, J., Liu, X. and Zhao, T. (2005), "Shear capacity of reinforced concrete columns strengthened with CFRP sheet", *J. Zhejiang Univ. SCIENCE*, **6A**(8), 853-858.
Yalcin, C., Kaya, O. and Sinangil, M. (2008), "Seismic retrofitting of R/C columns having plain rebars using CFRP sheets for improved strength and ductility", *Constr. Build. Mater.*, **22**, 295-307.
Yang, Y., Sneed, L.H., Morgan, A., Saiidi, M.S. and Belarbi, A. (2015a), "Repair of RC bridge columns with interlocking spirals and fractured longitudinal bars-an experimental study", *Constr. Build. Mater.*, **78**, 405-420.
Yang, Y., Sneed, L.H., Saiidi, M.S., Belarbi, A., Ehsani, M. and He, R. (2015b), "Emergency repair of an earthquake-damaged RC bridge column with fractured bars using externally bonded prefabricated laminates-an experimental study", *J. Compos. Struct.*, **133**, 727-738.
Yılmaz, N. and Avşar, Ö. (2013), "Structural damages of the May 19, 2011 Kütahya-Simav Earthquake in Turkey", *Nat. Hazard.*, **69**(1), 981-1001.
Yurdakul, Ö. and Avşar, Ö. (2015), "Structural repairing of damaged reinforced concrete beam-column assemblies with CFRPs", *Struct. Eng. Mech.*, **54**(3), 521-543.

CC

Notations

A_c = Gross section area of column
A_0 = Area of transverse reinforcement
b_w = Width of column
d = Effective height of the cross section
$d_{\max}$ = Maximum displacement of specimen for idealized bi-linear form
d_y = Yield displacement of specimen
E_f = Elasticity module of the fibrous polymer
f_c = Standard cylindrical concrete compressive strength at 28 days after casting
f_c^* = Standard cylindrical concrete compressive strength at the date of experiment
f_{ct} = Tensile strength of concrete
f_{yw} = Yield strength of transverse reinforcement
h/L = Aspect ratio
n = Number of stirrup arms at a section
N_d = Axial force
n_f = Fibrous polymer winding plate number in one side
s = Spacing of transverse reinforcement
s_f = Distance of the fibrous polymer band from axis to axis
t_f = Effective thickness for one plate of fibrous polymer
V_f = Contribution of the fibrous polymer to the shear strength
V_r = Shear strength of the column
V_y = Yield load of specimen
w_f = Width of the fibrous polymer band
ε_f = Effective unit elongation limit of the fibrous polymer
$\delta_{\max}$ = Maximum drift ratio of specimen for idealized bi-linear form
δ_y = Yield drift ratio of specimen